Application of incremental Gaussian mixture models for characterization of wind field data

J. PARK, K. SMARSLY, K. H. LAW and D. HARTMANN

ABSTRACT

Structural responses and power output of a wind turbine are strongly affected by the wind field acting on the wind turbine. Knowledge about the wind field and its variations is essential not only for designing, but also for cost-efficiently managing wind turbines. Wind field monitoring collects and stores wind field time series data. Over time the amount of data can be overwhelming. Furthermore, the correlation among the wind field statistical features is difficult to capture. Here, we explore the use of online machine learning to study the characteristics of wind fields, while effectively condensing the amount of monitoring data. In particular, incremental Gaussian mixture models (IGMM) are constructed to represent the joint probability density functions for wind field features, whose parameters are continuously updated as new data set is collected. The monitoring data recorded from an operating wind turbine in Germany is employed to test and compare the IGMM with conventional machine learning approach that uses an entire historical data set.

Nomenclature

U_{67}: mean value of a 20-minute wind speed time series data at 67 m height
U_{13}: mean of a 20-minute wind speed time series data at 13 m height
σ_{U67}: standard deviation of a 20-minute wind speed time series data at 67 m height
$\boldsymbol{x}^{(i)} = \left\{x_1^{(i)}, x_2^{(i)}, x_3^{(i)}\right\} = \{{U_{67}}^{(i)}, {U_{67}}^{(i)} - {U_{13}}^{(i)}, {\sigma_{U67}}^{(i)}\}$: feature vector for *i*-th wind field data set
$\boldsymbol{h}^t = \{\widehat{\boldsymbol{M}}, \widehat{\boldsymbol{\phi}}, \widehat{\boldsymbol{\mu}}, \widehat{\boldsymbol{C}}\}$: local Gaussian mixture models at time t
$\hat{M}_i$: number of data points classified as the ith Gaussian probability density function in $\boldsymbol{h}^t$
$\hat{\phi}_i$: weight for the i-th Gaussian probability density function in $\boldsymbol{h}^t$
$\widehat{\boldsymbol{\mu}}_i$: mean vector for the i-th Gaussian probability density function in $\boldsymbol{h}^t$
$\widehat{\boldsymbol{C}}_i$: covariance matrix for the i-th Gaussian probability density function in $\boldsymbol{h}^t$
$\boldsymbol{H}^t = \{\boldsymbol{M}^t, \boldsymbol{\phi}^t, \boldsymbol{\mu}^t, \boldsymbol{C}^t\}$: Global Gaussian mixture models at time t
M_i^t : number of data points classified as the i-th Gaussian probability density function in $\boldsymbol{H}^t$
ϕ_i^t : weight for the i-th Gaussian probability density function in $\boldsymbol{H}^t$
$\boldsymbol{\mu}_i^t$: mean vector for the i-th Gaussian probability density function in $\boldsymbol{H}^t$
$\boldsymbol{C}_i^t$: covariance matrix for the i-th Gaussian probability density function in $\boldsymbol{H}^t$

Jinkyoo Park, Department of Civil and Environmental Engineering, Stanford University, Stanford, CA, USA
Kay Smarsly, Department of Civil Engineering, Berlin Institute of Technology, Berlin, Germany
Kincho H. Law, Department of Civil and Environmental Engineering, Stanford University, Stanford, CA, USA
Dietrich Hartmann, Department of Civil and Environmental Engineering, Ruhr-Univ. Bochum, Bochum, Germany

INTRODUCTION

Wind field characteristics, varying with geographic locations and times, greatly affect the power output and structural responses of a wind turbine. Wind field characteristics are conventionally described by time averaged features, such as mean wind speed, turbulence intensity and power exponent which quantifies the steepness of the vertical mean wind profile. Different combinations of these features cause different responses from a wind turbine. For example, fast wind with high turbulence tends to cause high bending moment on the wind turbine tower while fast wind with steep shear profile tends to induce excessive fatigue damage on blades [1]. How wind field input features are correlated could provide insight to the load demand on a wind turbine.

Conventional structural monitoring typically records and stores the excitation and response time series data. Over time, large amount of monitoring data are collected and are difficult to manage. Recently, compressed sensing has been proposed to extract the features from the data that can then be used to reconstruct the time series. Wavelet transformation and L_2 regularization norm have been applied for compressed sensing [2, 3]. While focusing on condensation and reconstruction, compressed sensing does not provide insight into how to extract trends from the data.

In this study, we explore the use of incremental Gaussian mixture models to represent the wind field characteristic, in which data condensation and trend estimation are interwoven. The correlations among the time averaged wind field features as well as the probability of occurrence for a combination of certain wind features can be captured by a joint Gaussian probability density function. Since only a small number of parameters are needed to represent the trends in the data set, the amount of data to be retained can be significantly reduced. Furthermore, for IGMM, the parameters for Gaussian Mixture models are updated as new data set is collected. The method can potentially be useful for tracking the variation in the wind field characteristics.

A REFERENCE WIND TURBINE INVESTIGATED IN THIS STUDY

In this study, monitoring data is taken from a 500 kW wind turbine located in Germany. The wind turbine, in operation for about 15 years, has a hub height of 65 m and a rotor diameter of 40.3 m. A life-cycle management (LCM) framework has been installed on the wind turbine to continuously collect structural, environmental, and operational data. The framework consists of two major components, a SHM system and a set of interconnected software modules installed at spatially distributed locations [4]. The software modules include, for example, a monitoring database for persistent storage of the recorded data sets, a central server for automated data processing, a PC cluster for high-performance parallel computing, a management module supporting life-cycle analyses, and Internet-enabled user interfaces providing online access to authorized users and to external application programs [5]. Details on the software modules have previously been described elsewhere [6-8].

The wind turbine is installed with a structural health monitoring system comprising of a network of sensors, data acquisition units, and an on-site server [11]. The sensors (accelerometers, displacement transducers, and temperature sensors) are placed at different levels inside and outside the steel tower and on the foundation of the wind turbine. In addition, two anemometers are deployed to continuously measure

wind speed, wind direction, and air temperature. The first anemometer, a cup anemometer, is installed on the top of the wind turbine nacelle at the height of 67 m. The second anemometer, a three-dimensional ultrasonic anemometer, is mounted on a telescopic mast at 13 m height next to the wind turbine.

Three time averaged statistics of wind field data collected at the wind turbine site are used in this study:

- U_{67}: mean of a 20-minute wind speed time series at 67 m height
- U_{13}: mean of a 20-minute wind speed time series at 13 m height
- σ_{U67}: standard deviation of the 20-minute wind speed time series at 67 m height

The characteristics of the i-th wind field time series (20-min duration) is represented by a feature vector $\boldsymbol{x}^{(i)} = \left\{x_1^{(i)}, x_2^{(i)}, x_3^{(i)}\right\} = \{{U_{67}}^{(i)}, {U_{67}}^{(i)} - {U_{13}}^{(i)}, {\sigma_{U67}}^{(i)}\}$. The collection includes a total of 3,930 feature vectors $\boldsymbol{D} = \{\boldsymbol{x}^{(1)}, \dots, \boldsymbol{x}^{(3,930)}\}$ which are equally divided into 5 sets (i.e., $\boldsymbol{D} = \{\boldsymbol{D}^1, \dots, \boldsymbol{D}^5\}$), each of which having 786 feature vectors.

THEORY ON INCREMENTAL GAUSSIAN MIXTURE MODELS

The site-specific wind field characteristics are studied by constructing the joint probability function (PDF) $f(\boldsymbol{x})$ for the feature vector $\boldsymbol{x}$. The joint PDF for $\boldsymbol{x}$ is constructed based on Gaussian mixture models (GMM), where the joint PDF is expressed as a linear combination of K probability density functions [12]:

$$f(\boldsymbol{x}) = \sum_{j=1}^{K} \phi_j f_j(\boldsymbol{x}) = \sum_{j=1}^{K} \phi_j P(\boldsymbol{x}|\boldsymbol{\mu}_j, \mathbf{C}_j) \quad (1)$$

where $P(\boldsymbol{x}|\boldsymbol{\mu}_j, \boldsymbol{C}_j)$ is the j-th Gaussian probability density function (GPDF) with the mean vector $\boldsymbol{\mu}_j$ and covariance matirx $\mathbf{C}_j$, modeled by a multivariate normal distribution $N(\boldsymbol{\mu}_j, \mathbf{C}_j)$, and ϕ_j is the weight of the j-th GPDF. The number of GPDFs K, the set of weights $\boldsymbol{\phi} = \{\phi_1, \dots, \phi_K\}$, the set of mean vectors $\boldsymbol{\mu} = \{\boldsymbol{\mu}_1, \dots, \boldsymbol{\mu}_K\}$ and the set of covariacne matrices $\boldsymbol{C} = \{\boldsymbol{C}_1, \dots, \boldsymbol{C}_K\}$ are determined by those values that maximize the logliklihood of the data $\boldsymbol{D} = \{\boldsymbol{x}^{(1)}, \dots, \boldsymbol{x}^{(m)}\}$ using the "Expected Maximization (EM) Algorithm" described in [12].

In this study, the parameters for the GMM are updated and repesented by the increamental Gaussian mixture models (IGMM) [13-15]. When new data $\boldsymbol{D}^t = \{\boldsymbol{x}^{(1)}, \dots, \boldsymbol{x}^{(m^t)}\}$, where m^t = 786 in this case, arrives at time t, the local GMM $\boldsymbol{h}^t = \{\widehat{\boldsymbol{M}}, \widehat{\boldsymbol{\phi}}, \widehat{\boldsymbol{\mu}}, \widehat{\boldsymbol{C}}\}$ is constructed. The local GMM $\boldsymbol{h}^t$ consists of K_h GPDFs (i.e., $\boldsymbol{h}^t = \{\boldsymbol{h}_1^t, \dots, \boldsymbol{h}_{K_h}^t\}$, where the i-th GPDF is denoted by $\boldsymbol{h}_i^t = \left\{\widehat{M}_i, \hat{\phi}_i\, \widehat{\boldsymbol{\mu}}_i, \widehat{\boldsymbol{C}}_i\right\}$). The number K_h and the corresponding parameter sets, $\widehat{\boldsymbol{\phi}} = \left\{\hat{\phi}_1, \dots, \hat{\phi}_{K_h}\right\}$, $\widehat{\boldsymbol{\mu}} = \{\widehat{\boldsymbol{\mu}}_1, \dots, \widehat{\boldsymbol{\mu}}_{K_h}\}$ and $\widehat{\boldsymbol{C}} = \{\widehat{\boldsymbol{C}}_1, \dots, \widehat{\boldsymbol{C}}_{K_h}\}$ are determined based on the EM algorithm. In addition, $\widehat{\boldsymbol{M}} = \{\widehat{M}_1, \dots, \widehat{M}_{K_h}\}$ denotes the number of data points classified to each local GPDF. That is, $\widehat{M}_i$ is the number of data points believed to be drawn from the i-th local GPDF $\boldsymbol{h}_i^t$. The local GMM $\boldsymbol{h}^t$ captures the distribution only in the current data $\boldsymbol{D}^t$.

Global GMM $\boldsymbol{H}^t = \{\boldsymbol{M}^t, \boldsymbol{\phi}^t, \boldsymbol{\mu}^t, \boldsymbol{C}^t\}$ at time t is constructed by merging the the local GMM $\boldsymbol{h}^t = \{\widehat{\boldsymbol{M}}, \widehat{\boldsymbol{\phi}}, \widehat{\boldsymbol{\mu}}, \widehat{\boldsymbol{C}}\}$ at time t with the global GMM $\boldsymbol{H}^{t-1} = \{\boldsymbol{M}^{t-1}, \boldsymbol{\phi}^{t-1}, \boldsymbol{\mu}^{t-1}, \boldsymbol{C}^{t-1}\}$ at time $t-1$. The merging process occurs pairwise between each of the K_h GPDFs in $\boldsymbol{h}^t$ and each of the K_H GPDFs in $\boldsymbol{H}^{t-1}$. For example, when the i-th GPDF $\boldsymbol{H}_i^{t-1}$ in the global $\boldsymbol{H}^{t-1}$ and the j-th GPDF $\boldsymbol{h}_j^t$ in the local GMM $\boldsymbol{h}^t$ are similar, i.e., $N(\boldsymbol{\mu}_i^{t-1}, \boldsymbol{C}_i^{t-1}) \approx N(\widehat{\boldsymbol{\mu}}_j, \widehat{\boldsymbol{C}}_j)$, the two GPDFs are merged into the i-th GPDF $\boldsymbol{H}_i^t = \{M_i^t, \phi_i^t, \boldsymbol{\mu}_i^t, \boldsymbol{C}_i^t\}$ in the global GMM $\boldsymbol{H}^t$, whose parameters are given as follows [13]:

$$M_i^t = M_i^{t-1} + \widehat{M}_j \tag{2}$$

$$\phi_i^t = \frac{M_i^{t-1} + \widehat{M}_j}{\sum_{q=1}^{K_H} M_q^{t-1} + \sum_{q=1}^{K_h} \widehat{M}_q} \tag{3}$$

$$\boldsymbol{\mu}_i^t = \frac{1}{M_i^t}\left(M_i^{t-1}\boldsymbol{\mu}_i^{t-1} + \widehat{M}_j\widehat{\boldsymbol{\mu}}_j\right) \tag{4}$$

$$\begin{aligned}\boldsymbol{C}_i^t = &\frac{M_i^{t-1}}{M_i^{t-1}+\widehat{M}_j}\left(\boldsymbol{C}_i^{t-1} + (\boldsymbol{\mu}_i^{t-1} - \boldsymbol{\mu}_i^t)\,(\boldsymbol{\mu}_i^{t-1} - \boldsymbol{\mu}_i^t)^T\right) \\ &+ \frac{\widehat{M}_j}{M_i^{t-1}+\widehat{M}_j}\left(\widehat{\boldsymbol{C}}_j + (\widehat{\boldsymbol{\mu}}_j - \boldsymbol{\mu}_i^t)\,(\widehat{\boldsymbol{\mu}}_j - \boldsymbol{\mu}_i^t)^T\right)\end{aligned} \tag{5}$$

Note that M_i^t accumulates the number of data points that have been classified into the i-th GPDF in the global GMM $\boldsymbol{H}^t$, and the weight ϕ_i^t is computed based on the historical and the current parameters.

When a GPDF in $\boldsymbol{h}^t$ and a GPDF in $\boldsymbol{H}^t$ do not match, however, both GPDFs are included in $\boldsymbol{H}^t$ with updated weights. For example, if the i-th GPDF in $\boldsymbol{H}^{t-1}$ does not match any GPDFs in $\boldsymbol{h}^t$, the GPDF $\boldsymbol{H}_i^{t-1}$ remains in $\boldsymbol{H}^t$ with an updated weight $\phi_i^t = M_i^{t-1}/(\sum_{q=1}^{K_H} M_q^{t-1} + \sum_{q=1}^{K_h} \widehat{M}_q)$. If the j-th GPDF in $\boldsymbol{h}^t$ does not match any GPDFs in $\boldsymbol{H}^{t-1}$, $\boldsymbol{h}_j^t$ is added to $\boldsymbol{H}^t$ as the new j'-th GPDF with the weight $\phi_{j'}^t = \widehat{M}_j/(\sum_{q=1}^{K_H} M_q^{t-1} + \sum_{q=1}^{K_h} \widehat{M}_q)$ [13]. The global GMM $\boldsymbol{H}^t = \{\boldsymbol{M}^t, \boldsymbol{\phi}^t, \boldsymbol{\mu}^t, \boldsymbol{C}^t\}$, in a weak sense, accounts for the distribution of all historical data sets $\boldsymbol{D} = \{\boldsymbol{D}^1, \ldots, \boldsymbol{D}^t\}$. By incrementally updating the parameters of GMM, it may not be necessary to store the data set $\boldsymbol{D}^t$ in the LCM framework; the parameters of IGMM serve as a source for the statistical information used for updating the global GMM.

We evaluate the similarity between two GPDFs by using maximum mean discrepancy (MMD) measure [16], which is defined as

$$D(P, Q, \boldsymbol{F}) \stackrel{\text{def}}{=} \sup_{f \in \boldsymbol{F}}(E_{\boldsymbol{x}\sim P}[f(\boldsymbol{x})] - E_{\boldsymbol{x}\sim Q}[f(\boldsymbol{x})]) \tag{6}$$

where P and Q are two probability distributions, and $\boldsymbol{F}$ denotes a set of bounded continuous functions. Intuitively, if the probability distributions P and Q are similar, the expected values of a function in $\boldsymbol{F}$ evaluated with the samples drawn from the two distributions are likely close to each other. That is, a low MMD value reflects high similarity between the two distributions. We use MMD as a criterion for determining whether two GPDFs are to be merged. If P and Q are both Gaussian distributions,

empirical estimation of the MMD value can be easily calculated using Gaussian kernel function and sampled data points from the distributions, using the procedure described by Gretton et al. [16]. A similarity test based on MMD simplifies the conventional similarity test that separately checks the equality of mean vectors and covariance matrices [13]. The algorithm implemented for updating IGMM in this study can be summarized as follows.

Algorithm (Incremental Gaussian mixture model using maximum mean discrepancy measure)

INPUT: Global GMM $\boldsymbol{H}^{t-1} = \{\boldsymbol{M}^{t-1}, \boldsymbol{\phi}^{t-1}, \boldsymbol{\mu}^{t-1}, \boldsymbol{C}^{t-1}\}$ and new data $\boldsymbol{D}^t = \{\boldsymbol{x}^{(i)}, \dots, \boldsymbol{x}^{(m_t)}\}$
OUTPUT: Global GMM $\boldsymbol{H}^t = \{\boldsymbol{M}^t, \boldsymbol{\phi}^t, \boldsymbol{\mu}^t, \boldsymbol{C}^t\}$
Apply EM algorithm to estimate local GMM $\boldsymbol{h}^t = \{\widehat{\boldsymbol{M}}, \widehat{\boldsymbol{\phi}}, \widehat{\boldsymbol{\mu}}, \widehat{\boldsymbol{C}}\}$ for the data set D^t
for each GPDF *i* in $\boldsymbol{H}^{t-1}$ **do**
  Generate sample $\boldsymbol{S}^i \sim N(\boldsymbol{\mu}_i^{t-1}, \boldsymbol{C}_i^{t-1})$
  for each GPDF *j* in $\boldsymbol{h}^t$ **do**
    Generate sample $\boldsymbol{S}^j \sim N(\widehat{\boldsymbol{\mu}}_j, \widehat{\boldsymbol{C}}_j)$
    Calculate maximum mean discrepancy MMD between $\boldsymbol{S}^i$ and $\boldsymbol{S}^j$
    if MMD is lower than a certain threshold
      Merge the *i*-th GPDF in $\boldsymbol{H}^{t-1}$ and the *j*-th GPDF in $\boldsymbol{h}^t$
    end if
  end for
end for
for each remaining GPDF *i* in $\boldsymbol{H}^{t-1}$ **do**
  Assign the *i*-th GPDF of $\boldsymbol{H}^{t-1}$ to H^t with updated weight
end for
for each remaining GPDF *j* in $\boldsymbol{h}^t$ **do**
  Assign the *j*-th GPDF of $\boldsymbol{h}^t$ to $\boldsymbol{H}^t$ with updated weight
end for

APPLICATION OF INCREMENTAL GAUSSIAN MIXTURE MODELS

The incremental GMM is applied to a data set consisting of 3,930 wind field data points that have been collected during the daytime operation of a wind turbine. For testing the incremental updating procedure, the data is divided into 5 data sets with 786 data points each. Upon receiving new data set $\boldsymbol{D}^t$, the new global GMM $\boldsymbol{H}^t$ is constructed using the previous global GMM $\boldsymbol{H}^{t-1}$ and the local GMM $\boldsymbol{h}^t$ constructed from $\boldsymbol{D}^t$. Figure 1 shows the updated GMMs at different times in terms of three marginal PDFs $f_{X_1,X_2}(x_1, x_2), f_{X_2,X_3}(x_2, x_3)$ and $f_{X_1,X_3}(x_1, x_3)$ ($x_1 = U_{67}, x_2 = U_{67} - U_{13}$ and $x_3 = \sigma_{U67}$), which are represented as contour lines. In the figures, the new data points in $\boldsymbol{D}^t$ are represented as circles, while the historical data points in $\{\boldsymbol{D}^1, \dots, \boldsymbol{D}^{t-1}\}$ are shown as crosses even though these historical data points are not used for construting global GMM by the incremental approach.

The constructed PDF reflects the site and time specific wind field characteristics, and can be possibly used to infer how wind turbine loads and power are distributed. That is, we can indirectly find the distributions of loads and power since wind turbine loads and power can be estimated from a combination of wind input features. Furthermore, the variations in the shape of PDF indicate the temporal variation in wind field characteristics, which can be tracked by IGMM. Figure 1 shows that the updated GMM captures well not only the trend for local data points (circles), but also the historical data points (crosses). In addition, the PDF contour lines become smoother as historical GMM information is accumulated. The figures also show that

U_{67} and σ_{U67}, the mean and the standard deviation of wind speed time series collected at 67 m height, are in a strong linear relationship.

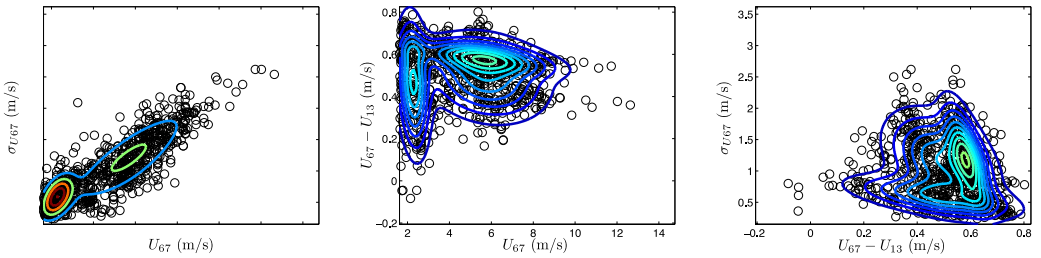

(a) Marginal PDFs given $\boldsymbol{D}^1$.

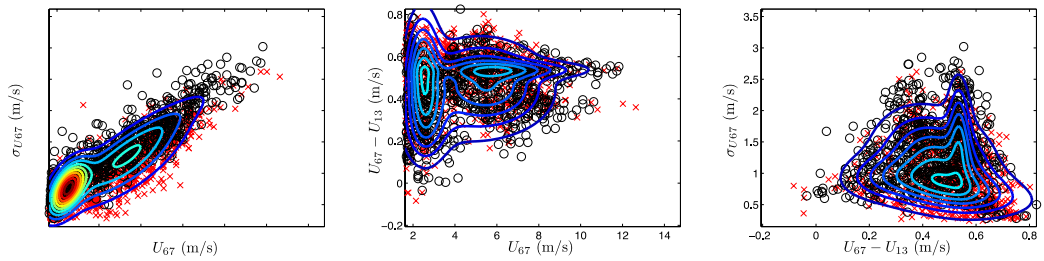

(b) Marginal PDFs given $\boldsymbol{H}^1$ and $\boldsymbol{D}^2$.

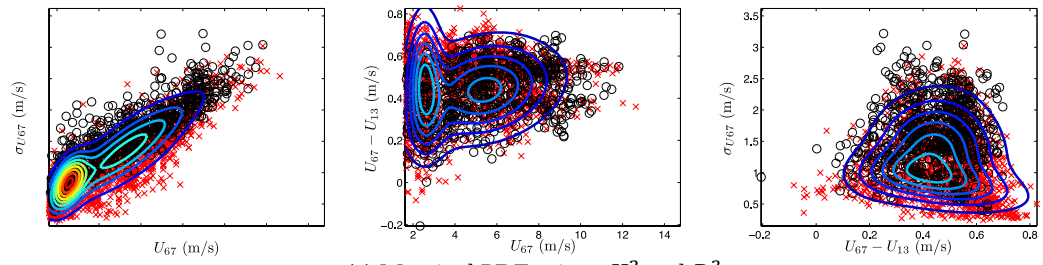

(c) Marginal PDFs given $\boldsymbol{H}^2$ and $\boldsymbol{D}^3$.

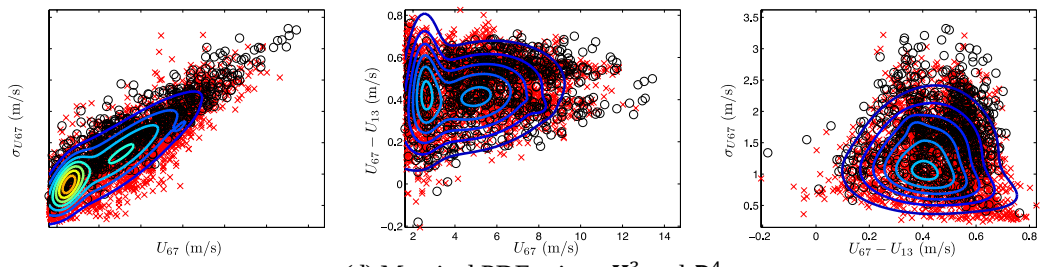

(d) Marginal PDFs given $\boldsymbol{H}^3$ and $\boldsymbol{D}^4$.

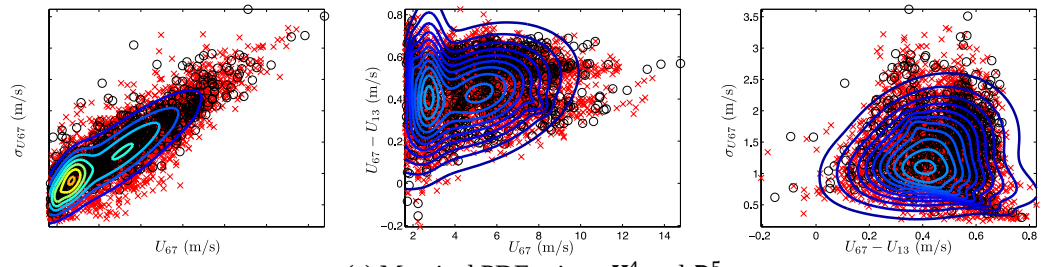

(e) Marginal PDFs given $\boldsymbol{H}^4$ and $\boldsymbol{D}^5$.

Figure 1. Illustration of the incremental Gaussian mixture model algorithm: The marginal PDFs are constructed using the preserved parameters $\boldsymbol{H}^{t-1}$ and the newly measured data sets $\boldsymbol{D}^t$ at time t.

The effectiveness of IGMM can be evaluated by comparing the log-likelihood of the data, which is expressed as:

$$l(\boldsymbol{\phi}, \boldsymbol{\mu}, \boldsymbol{C}) = \sum_{i=1}^{m} \log P\left(\boldsymbol{x}^{(i)} | \boldsymbol{\phi}, \boldsymbol{\mu}, \boldsymbol{C}\right) = \sum_{i=1}^{m} \log P\left(\boldsymbol{x}^{(i)} | \boldsymbol{\mu}, \boldsymbol{C}\right) \log P\left(z^{(i)} | \boldsymbol{\phi}\right) \quad (7)$$

where $z^{(i)}$ denotes the GPDF where $\boldsymbol{x}^{(i)}$ is assumed to be drawn. Since the value of the log-likelihood is negative ($P\left(\boldsymbol{x}^{(i)} | \boldsymbol{\phi}, \boldsymbol{\mu}, \boldsymbol{C}\right) \leq 1$), it may be more convenient to use the negative value of the log-likelihood (the lower negative log-likely hood is the higher probability is) for comparison purpose. Figure 2 compares the negative of log-likelihood of the data sets $\{\boldsymbol{D}^1, \ldots, \boldsymbol{D}^t\}$ using three different approaches in constructing the GMMs: (1) a batch GMM that uses all historical data sets $\{\boldsymbol{D}^1, \ldots, \boldsymbol{D}^t\}$ in modeling the PDF; (2) the incremental GMM that uses the current data set $\boldsymbol{D}^t$ and the preserved global GMM $\boldsymbol{H}^{t-1}$ and (3) the "no history data" model that uses only current data set $\boldsymbol{D}^t$. The "no history data" model has the lowest log-likelihood, because the GMM captures the trend using only the current data set. The incremental GMM performs better than the "no history data" model since it preserves the historical distribution information. Since IGMM uses only the current data sets and the significantly condensed historical distribution information, the effectiveness decreases as the number of data sets increases when comparing with the batch GMM approach which uses all the prior data in the GMM.

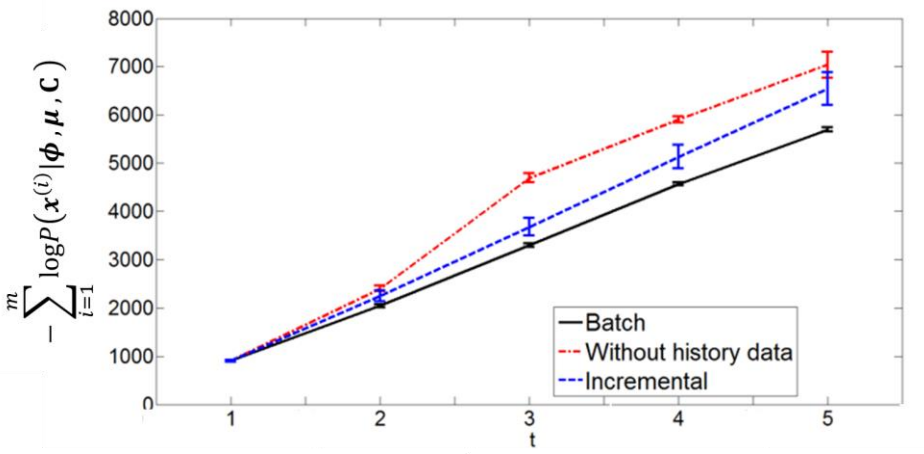

Figure 2. Comparison of the log-likelihood of the data sets; 100 simulations are conducted and the mean and standard deviation are compared.

SUMMARY AND CONCLUSIONS

This study explores the use of incremental Gaussian mixture model to characterize the daytime wind field data collected from a 500 kW wind turbine located in Germany. The joint probability density function constructed from Gaussian mixture model shows how the wind speeds and the level of turbulence are distributed. Since the time averaged wind turbine loads and power are strongly dependent on the wind field input feature vector, the correlations among the wind field features and the estimated probability for a certain wind field can potentially be used to predict loading effects and power of a wind turbine. By incrementally updating the parameters for GMM, the amount of data need to be stored in the monitoring framework can be

significantly reduced. The performance of IGMM is likely dependent on the size of the data sets, used for updating the GMM. Our future investigation will explore the tradeoff between the effectiveness of IGMM and the number and size of data sets.

ACKNOWLEDGEMENTS

The wind turbine monitoring activities were partially funded by the German Research Foundation (DFG) through the grants SM 281/1-1, SM 281/2-1, and HA 1463/20-1. Any opinions, findings, conclusions, or recommendations are those of the authors and do not necessarily reflect the views of the DFG.

REFERENCES

1. Park, J, Manuel, L. and Basu, S. 2012. "Toward Understanding Characteristics of the Stable Boundary Layer that Influence Wind Turbine Loads," Proc. 50th AIAA Aerospace Sciences Meeting including the New Horizons Forum and Aerospace Exposition, 01/9/2012.
2. Bao, Y, Beck, J. and Li, H. 2011. "Compressive sampling for accelerometer signals in structural health monitoring," Structural Health Monitoring, 10(3): 235-246
3. Huang, Y, Beck, J., Li, H. and Wu, S. 2011. "Robust diagnostics for Bayesian compressive sensing with applications to structural health monitoring," Proc. SPIE 7982, Smart Sensor Phenomena, Technology, Networks, and Systems, 04/15/2011.
4. Smarsly, K., Hartmann, D. and Law, K.H., 2013. "An Integrated Monitoring System for Life-Cycle Management of Wind Turbines," International Journal of Smart Structures and Systems (in press).
5. Smarsly, K., Law, K.H. and Hartmann, D., 2011. "Implementation of a multiagent-based paradigm for decentralized real-time structural health monitoring," Proceedings of the 2011 ASCE Structures Congress. Las Vegas, NV, USA, 04/14/2011.
6. Law K.H., Smarsly, K. and Wang, Y., 2013. "Sensor Data Management Technologies," In: Wang, M. L., Lynch, J. P. and Sohn, H. (eds.). Sensor Technologies for Civil Infrastructures: Performance Assessment and Health Monitoring. Sawston, UK: Woodhead Publishing, Ltd. (in press).
7. Smarsly, K., Law, K.H. and Hartmann, D., 2011. "Implementing a Multiagent-Based Self-Managing Structural Health Monitoring System on a Wind Turbine," Proceedings of the 2011 NSF Engineering Research and Innovation Conference. Atlanta, GA, USA, 01/04/2011.
8. Smarsly, K., Law, K.H. and Hartmann, D., 2013. "A cyberinfrastructure for integrated monitoring and life-cycle management of wind turbines," Proceedings of the 20th International Workshop on Intelligent Computing in Engineering. Vienna, Austria, 06/30/2013.
9. Hartmann, D., Smarsly, K. and Law, K.H., 2011. "Coupling Sensor-Based Structural Health Monitoring with Finite Element Model Updating for Probabilistic Lifetime Estimation of Wind Energy Converter Structures, "Proceedings of the 8th International Workshop on Structural Health Monitoring 2011. Stanford, CA, USA, 09/13/2011.
10. Smarsly, K. and Hartmann, D., 2010. "Agent-Oriented Development of Hybrid Wind Turbine Monitoring Systems," Proceedings of ISCCBE International Conference on Computing in Civil and Building Engineering. Nottingham, UK, 06/30/2010.
11. Lachmann, S., Baitsch, M., Hartmann, D. and Höffer, R. 2009. "Structural lifetime prediction for wind energy converters based on health monitoring and system identification," Proceedings of the 5th European & African Conference on Wind Engineering. Florence, Italy, 07/19/2009.
12. Render, A.R., and Walker, F.H. 1984. "Mixture Densities, Maximum Likelihood and the EM Algorithm," SIAM Review, 26(2):195-239.
13. Song, M., and Wang, H. 1996. "Highly efficient incremental estimation of Gaussian mixture models for online data stream clustering," Proceedings of the SPIE 5803, Intelligent Computing: Theory and Applications III, 174, 08/05/2005.
14. Declercq, A. and Piater, H. J. 2008. "Online learning of Gaussian mixture models: a two-level approach," Proc. of the Third International Conference on Computer Vision Theory and Applications, 01/22/2008.
15. Stauffer, C. and Grimson, W. 1999. "Adaptive background mixture models for real-time tracking," In Computer Vision and Pattern Recognition, 2: 252–258
16. Gretton, A., Borgwardt, K.M., Rasch, M., Scholkopf, B., and Smola, A.J. 2007. "A Kernel Approach to Comparing Distributions," Proceedings of the 22nd national conference on Artificial intelligence, 07/22/2007.